# Studies of the Gas Tori of Titan and Triton

William H. Smyth

and

M. L. Marconi

Atmospheric and Environmental Research, Inc.
840 Memorial Drive
Cambridge, MA 02139-3794

July 23, 1997

Final Report for the Period
January 24, 1994 to July 23, 1997

## TABLE OF CONTENTS

# I. INTRODUCTION

The general objective of this project is to advance our theoretical understanding of gas tori for the outer planet satellites and hence to enhance our ability to interpret observational data and to make available key concepts or quantitative results that are relevant to a number of other related theoretical studies. These studies are important to connect the aeronomy and photo- and ion chemistry of satellite atmospheres and their predicted gas loss rates, the evolution and distributions of gases in the larger planetary environment, and the ion loading and other impacts of these gases on the composition, structure, and properties of the planetary magnetospheres. Central objectives of this project are to explore for the satellites Titan and Triton the effects of two new mechanisms that we have very recently discovered (Smyth and Marconi 1993) to operate on gas tori in the outer planet satellite systems. These two mechanisms can dramatically alter the current picture that has been widely adopted for the structure and evolution of long-lived gas tori (i.e., lifetime long enough to achieve approximate azimuthal symmetry about the planet) and, in particular, have profound consequences on the interpretation of Voyager data for both neutral and ionized species in the circumplanetary environments of Saturn and Neptune. Due, however, to the substantially reduced budget available for this project, the primary emphasis of the research was focused on the Titan component, with a limited effort (as time permitted) expended on the Triton component.

For the Saturn system, comparable amounts of thermal H and $H_2$ and a much smaller amount of nonthermal N are thought to escape Titan and form gas tori. These tori are thought to be essentially collisionless because the lifetime loss processes of these gases in the moderate Saturn magnetosphere, although slow, are sufficiently rapid to avert collisional conditions. For the atomic hydrogen torus, the perturbation of solar radiation pressure experienced by H atoms as they resonance scatter Lyman-$\alpha$ photons --- the first new mechanism --- was shown by Smyth and Marconi (1993) to be operative and to destroy the normally assumed cylindrical symmetry of the torus produced by the 1/r central potential of a planet. This new mechanism causes H atom orbits to evolve inward as their eccentricities increase, and a significant fraction of these atoms is lost from the torus (having a preferred orientation of their perigee-axes) by colliding with the planet near its dusk side before they are otherwise lost through lifetime processes. This time evolution for a typical H atom lost from Titan is shown in Figure 1. Solar radiation pressure thus provides a natural mechanism for understanding the asymmetric distribution of hydrogen about Saturn recently reported by Shemansky and Hall (1992). This new understanding will subsequently allow the current question of the consistency of this atomic hydrogen distribution with the composition and properties of the inner magnetospheric plasma and the inner icy satellite tori to be addressed more clearly. In contrast to atomic hydrogen, $H_2$ and N will escape Titan and form approximately azimuthally symmetric tori about Saturn (i.e., the traditionally

adopted torus picture) since, for both species, solar radiation pressure is not important and the loss by lifetime processes is sufficiently long to achieve symmetry. The study in this project has been limited to the spatial nature the H gas tori of Titan to explore the consequences of the new "solar radiation pressure mechanism" noted above.

For the Neptune system, comparable amounts of H and $H_2$ and N are thought to escape thermally from Triton and form gas tori. The lifetimes of these three gases in the magnetosphere of Neptune are, however, very long and are comparable to their photo-lifetimes because of the low plasma density and the small fraction of time that the tori spend in the more dense regions of the magnetosphere which executes complex motion about the planet. Because of these long lifetimes, the density of each torus will be collisional, and the neutral-neutral collision time will be shorter than all other time scales except for the typical Kepler orbit period of the atom or molecule (see Table 1 in Smyth and Marconi 1993). The collisional nature of the three gases will cause the multi-species gas torus to dynamically evolve in an inherently nonlinear manner that will depend upon the 1/r nature of the potential of the planet. This collisional evolution will cause the gas torus to expand both inwardly (leading to inward gas loss by collision with the planet's atmosphere) and outwardly (leading to volume dilution and outward gas loss by escape from the planet). This expansion mechanism, the second new mechanism noted above, is a non-linear effect that has been known for two decades in the field of solar system and ring formation but has been previously overlooked as important until now for the field of collisional gas tori about planets (Smyth and Marconi 1993). The final structure and density of the gas torus of Triton are particularly important in understanding the plasma sources recently identified in the analysis of the Voyager PLS data for the Neptune magnetosphere. This fascinating new expansion mechanism for the multi-species collisional gas torus of Triton provides a challenging dynamical evolution problem. Due to the reduced budget support available for this project, the solution of this problem to be undertaken in this project for Triton will be diminished in scope. The Triton component has been initiated only in this project with the limited resources focused on the initial phases of the development of a Direct Simulation Monte Carlo (DSMC) model to describe the collisional physics of the gas species in the circumplanetary volume.

## II. STUDIES FOR THE TITAN TORUS

### 2.1 Model Description

The basic model for the spatial distribution and Lyman-$\alpha$ brightness of hydrogen in the Saturn system has been developed in the second and third project year. The model supports a central planetary source, an interior (combined inner icy satellite and ring) source, and a Titan source. For all sources, a choice of a monoenergetic, Maxwell Boltzmann, or a sputtering initial velocity distribution

is possible. For the Saturn source, a sunlit hemispherical source is assumed and includes the spin rate and obliquity of the planet. For the composite interior source, a point source moving on a circular orbit about Saturn is used where the radial position of the orbit may be varied between 2 and 15 Saturn radii ($R_S$). For the Titan source, a point source moving on a circular orbit about Saturn of radius 20.26 $R_S$ is adopted, and the effect of the satellite's gravity on the initial exobase source velocity distribution is also included. The model calculates the density and brightness of hydrogen by following the time evolving trajectories of many H atom orbits initially emitted from the sources. The trajectories are calculated using the computationally efficient orbital element method discussed by Smyth and Marconi (1993) and dynamically include Saturn's spherical gravity, the leading nonspherical $J_2$ planetary component, and solar radiation pressure acceleration. Loss processes for the H atoms include reactions with the planetary magnetosphere and solar wind plasmas, collisional loss with Saturn and its rings, and escape of sufficiently energetic H atoms from the planetary system. The model of the Saturnian magnetosphere adopted in calculating the spatially nonuniform electron impact and charge exchange lifetimes for hydrogen is that of Richardson and Sittler (1990) and Richardson (1995).

## 2.2 Observational Data for H

The three best observations to date of the H distribution in the Saturn system were published by Shemansky and Hall (1992): (1) a Voyager 1 preencounter UVS scan providing an approximately in the satellite plane dawn to dusk Lyman-α brightness profile acquired in 1980 during the period day of year (DOY) 239 to 256, (2) a Voyager 2 preencounter UVS scan providing an approximately in the satellite plane dawn to dusk Lyman-α brightness profile acquired in 1981 during the period DOY 180 to 186, and (3) a Voyager 1 postencounter UVS Lyman-α brightness mosaic image with the line of sight intersecting the satellite orbit plane at an angle of about 26° looking down on the north pole of the planet acquired in 1980 during the period DOY 324 to 343. These observations show, in contrast to earlier reported Voyager data (Broadfoot et al. 1981; Sandel et al. 1982), that (1) there is no evidence for an absence of hydrogen in the radial interval inside of ~8 $R_S$, but rather there is a peak in the Lyman-α intensity near the planet, and (2) there is no significant peak of Lyman-α intensity centered near Titan orbit as would be expected (Smyth 1981) based upon an azimuthally symmetric (doughnut) shaped hydrogen torus, but rather there is a local time asymmetry in the Lyman-α intensity distribution with the preencounter scans showing a preponderance of emission on the dawnside of the system whereas the postencounter mosaic image data show more emission on the duskside. A reconciliation offered by Shemansky and Hall (1992) for the two different behaviors of the local time asymmetry was that the H distribution must have a complex three-dimensional morphology. Since at that time the satellite source was thought to produce an azimuthally symmetric H torus [the local time effect introduced by solar radiation acceleration (Smyth and Marconi 1993) had not yet been published], the

explanation for the nonuniformity in the local time distribution could only be attributed to a nonspherical Saturn source by Shemansky and Hall (1992). Model calculations undertaken in this project and discussed below which now include solar radiation acceleration, however, naturally produce a local time asymmetry in the circumplanetary H distribution for satellite sources and can fit the local time structures of the observations without a Saturn source.

## 2.3 Model Calculations

Modeling studies for the most definitive description of the spatial distribution of atomic hydrogen in the Saturn system discussed above and published by Shemansky and Hall (1992) have been undertaken and successfully completed in this project. These modeling studies are presented in a paper (Marconi and Smyth 1997) included in the Appendix. Only an overview summary of the major results and conclusions will therefore be presented below.

The contribution of a Titan source to the preencounter UVS dawn to dusk scan Lyman-$\alpha$ brightness profile acquired by the Voyager 2 spacecraft in 1981 during the period DOY 180 to 186 is shown in Figure 1 by the solid line. An isotropic satellite exobase source strength of $4.8 \times 10^{27}$ H atoms $s^{-1}$ was assumed for a Maxwellian velocity distribution with an exobase temperature of 186 K. Because of solar radiation acceleration, the double-humped Titan source profile is asymmetric and higher on the dawn side (left side). The profile is able to fit the observed Lyman-$\alpha$ brightness at larger distances (beyond about 20 $R_S$), but is not able to fit the much brighter emission at smaller distances from the planet. An additional source of H atoms closer to Saturn and within Titan's orbit at 20.26 $R_S$ is clearly required. The Lyman-$\alpha$ brightness profile, produced by combining an interior point source located on a circular orbit at 8.7 $R_S$ which corresponds to the orbital position of the icy inner satellite Rhea and the same Titan source adopted in Figure 1, is shown in Figure 2 and compared to the same Voyager 2 observation shown in Figure 1. The interior source is characterized by a 40,000 K Maxwellian velocity distribution, and its source strength is $1.9 \times 10^{28}$ H atoms $s^{-1}$, a factor of about 4 times larger than the Titan source. The contribution of the interior source is asymmetric and larger on the duskside of Saturn (right), opposite in since to the Titan source, and the combined interior and Titan sources fit the Voyager 2 observation in Figure 2 very well given the scatter in the data.

A very good fit to the Voyager 1 preencounter UVS scan providing an approximately in the satellite plane dawn to dusk Lyman-$\alpha$ brightness profile acquired in 1980 during the period day of year (DOY) 239 to 256 is also achieved by using a combined interior source and a Titan source as shown in Figure 3. The best fit (solid line) was achieved for a slightly smaller Titan source of $3.3 \times 10^{27}$ H atoms $s^{-1}$ with a 186 K Maxwellian velocity distribution at the satellite exobase and a slightly smaller

interior source located on a circular orbit at 8.7 $R_S$ with a source strength of $1.4 \times 10^{28}$ H atoms $s^{-1}$, still a factor of about 4 times larger than the Titan source.

Assuming the same Titan source and interior source as in Figure 3, a model calculation for the Voyager 1 postencounter UVS Lyman-$\alpha$ brightness mosaic image with the line of sight intersecting the satellite orbit plane at an angle of about 26° looking down on the north pole of the planet acquired in 1980 during the period DOY 324 to 343 has also been undertaken and is shown in Figure 4. Although there is substantial noise in the mosaic image, the only definite patterns evident is that both the model and observation are moderately brighter in the upper half of the ellipse defined by Titan's orbit (dotted line). It also appears that the overall magnitude of brightness variation is similar and that in both cases there appears to be a bright spot near the left hand apex of the satellite orbit. Within the limitations of the observations and the simplicity of the interior source adopted in the model, it would appear that the model and observation are broadly consistent.

In order to test the effect of an interior source, a number of model runs were constructed with the interior source placed at different locations ranging from 3 to 15 $R_S$. It was found that only if the source was placed in the neighborhood of 8 $R_S$ was a satisfactory fit to the observations in Figures 2 and 3 achieved. This should not be interpreted as implying that the major source of hydrogen is in the neighborhood of Rhea's orbital location. The precise distribution of the interior source is not well determined by the observations other than it must be largely confined inside of 8 or 9 $R_S$. As for the interior source velocity distribution for hydrogen, a large number of different initial velocity distributions were tried including other Maxwellian with different temperatures as well as sputtering distributions. It was found that any distribution with a characteristic energy that was not too small (not much less than about 1 eV), could be combined with the canonical Titan source (used above) to produce a profile which was in reasonable agreement with the observations in Figures 2 and 3. The actual source of H is likely to have a complex velocity distribution since there are several different possible sources for hydrogen.

The hydrogen source rates for the interior source above imply an $H_2O$ production rate of ~7-10 $\times 10^{27}$ molecules $s^{-1}$ assuming H is created from $H_2O$ and OH, with OH also produced mainly from $H_2O$. If the dominant source of H is sputtering from icy surfaces with comparable amounts of H and $H_2$ also liberated, then this $H_2O$ production rate could be reduced by a factor of 2 or 3 to a few $\times 10^{27}$ molecules $s^{-1}$. This lower $H_2O$ production rate is still a factor of two or three higher than the updated maximum total sputtered rate given by Shi et al. (1995) for an interior source, although other sources such as micrometeoroids, not included in these estimates, may also contribute. The larger $H_2O$ production rate of ~7-10 $\times 10^{27}$ molecules $s^{-1}$ could be consistent with estimates for the atomic oxygen

loss rate of 3 x$10^{27}$ atoms $s^{-1}$ within 4.5 $R_S$ of the planet by Shemansky and Hall (1992), if a comparable rate of loss occurs between 4.5 $R_S$ and the outer portion of our interior source at about 9 $R_S$. The lower $H_2O$ production rate of a few x$10^{27}$ molecules $s^{-1}$ is, however, consistent with the amount of OH detected by Shemansky et al (1993) at 4.5 $R_S$ as well as the amount of OH reported near Saturn's rings by Hall et al. (1996).

Model calculations for a Saturn source of H were also undertaken with the result that Saturn is only a minor contributor at least outside of the immediate location of the planet where the error bars in the data in Figures 2 and 3 are rather large. The different local time behaviors of the Triton source and the interior source produced by the acceleration of hydrogen by solar radiation pressure appear sufficient to reproduce the observations presently available. There is, however, current work in progress to further reduce these Voyager observations for hydrogen in the Saturn system (Herbert 1997), and it is anticipated that this effort will eventually permit a more incisive comparison of the models and observations.

## II. STUDIES FOR THE TRITON TORUS

The development of a model for the collisional evolution of gas tori in the Neptune system for given Triton sources was originally proposed to be undertaken by generalizing the numerical simulation method of Trulsen (1972). In this project, however, an improved numerical approach has been identified. This improved approach briefly discussed below is called Direct Simulation Monte Carlo (DSMC) as developed by Bird (1963), and effectively solves the non-linear collisional kinetic equation problem for a gas. Because of the limited resources available for this project, efforts have only been able to be focused on the initial phases of the development of a two-dimensional, multi-species DSMC model to describe the collisional physics of the gas species in the circumplanetary volume of Neptune. Progress in this development is summarized below.

The determination of the evolution and steady state of the quasicollisional gas in the Titan torus is a difficult and relative unexplored problem. In order to accomplish this task, we have selected the DSMC approach which has a proven history of application to complex rarefied gas flow problems in the field of Aeronautics. In addition, contemporary DSMC techniques have attained a high degree of refinement and have been adapted to function on parallel computers. Because of these factors, we have opted to employ DSMC rather than the much less efficient and less general method of Trulsen. We have been developing a spatially two-dimensional DSMC model for multi-species, chemically reacting, quasicollisional gases in a gravitational field. Since the Triton torus problem is highly demanding of computational resources, the model has been constructed to operate on parallel

computers so that the most powerful platforms can be brought to bear on the problem. At present the most basic elements of the model are completed and undergoing testing. In order, however, to apply this model to the Triton torus, several problem specific adaptations are necessary. These include the insertion of the Triton torus chemistry into the model and an appropriate Tritonogenic neutral gas source. Both of these tasks, although relatively straightforward, could not be completed with the limited resources available in this project and will be undertaken in a continuation of the Triton component of this project to be funded by the NSF Planetary Astronomy Program.

## REFERENCES


Bird, G. A. (1963) Approach to Equilibrium in a Rigid Sphere Gas, Phys. Fluids 6, 1518-1519.

Broadfoot, A.L., Sandel, B.R., Shemansky, D.E., Holberg, J.B., Smith, G.R., Strobel, D.F., McConnell, J.C., Kumar, S., Hunten, D.M., Atreya, S.K., Donahue, T.M., Moos, H.W., Bertaux, J.L., Blamont, J.E., Pomphrey,.R.B., and Linick, S. (1981) Ultraviolet Observations from Voyager I Encounter with Saturn, Science 212, 206-211.

Hall, D.T., Feldman, P.D., Holberg, J.H., and McGrath, M.A. (1996) Fluorescent Hydroxyl Emissions from Saturn's Ring Atmosphere, Science 272, 516-518.

Herbert, F. (1997) private communication.

Marconi, M.L. and Smyth, W.H. (1997) A Study of Hydrogen in the Saturnian System, Ap.J., submitted.

Richardson, J.D. (1995) An Extended Plasma Model for Saturn, Geophys. Res. Letts. 22, 1177-1180.

Richardson, J.D. and Sittler, E.C. (1990) A Plasma Density Model for Saturn Based on Voyager Observations, J. Geophys. Res. 95, 12019-12031.

Sandel, B.R., Shemansky, D.E., Broadfoot, A.L., Holberg, J.B., Smith, G.R., McConnell, J.C., Strobel, D.F., Atreya, S.K., Donahue, T.M., Moos, H.W., Hunten, D.M., Pomphrey, R.B., and Linick, S. (1982) Extreme Ultraviolet Observations from Voyager 2 Encounter with Saturn, Science 215, 548-553.

Shemansky, D.E. and Hall, D.T. (1992) The Distribution of Atomic Hydrogen in the Magnetosphere of Saturn, J. Geophys. Res. 97, 4143-4161.

Shemansky, D.E., Matheson, P., Hall, D.T., Hu, H.-Y., and Tripp, T.M. (1993) Detection of the Hydroxyl Radical in the Saturn Magnetosphere, Nature 336, 329-331.

Shi, M., Baragiola, R.A., Grosjean, D.E., Johnson, R.E., Jurac, S., and Schou, J. (1995) Sputtering of Water Ice Surfaces and Production of Extended Atmospheres, J. Geophys. Res. 100, 26387-26395.

Smyth, W.H. (1981) Titan's Hydrogen Torus, Ap.J. 246, 345-353.

Smyth, W. H. and Marconi, M. L. (1993) The Nature of the Hydrogen Tori of Titan and Triton, Icarus 101, 18-32.

Trulsen, J. (1972) Numerical Simulation of Jetstreams I: The Three Dimensional Case, Astrophys. Space Sci. 128, 3-20.

## FIGURE CAPTIONS

**Figure 1. Comparison of Model Calculated and Observed Lyman-α Brightness for a Titan Source Only.** The observed preencounter Lyman-α brightness of hydrogen for a dawn to dusk approximately radial scan as measured by the Voyager 2 spacecraft in 1981 between day of year (DOY) 180 and 186 and presented by Shemansky and Hall (1992) is compared to a model calculation (solid line) for a Titan source only. The Titan hydrogen source is characterized by a 186 K Maxwell-Boltzmann velocity distributed at the satellite exobase and an isotropic source strength of $4.8 \times 10^{27}$ H atoms $s^{-1}$.

**Figure 2. Comparison of Model Calculated and Observed Lyman-α Brightness for a Titan and Interior Source.** The observed preencounter Lyman-α brightness of hydrogen for a dawn to dusk approximately radial scan as measured by the Voyager 2 spacecraft in 1981 between day of year (DOY) 180 and 186 and presented by Shemansky and Hall (1992) is compared to a model calculation (solid line) including both a Titan source and an interior source. The Titan hydrogen source is the same as in Figure 1. The interior point source is located on a circular radius of 8.7 planetary radii from the planet and is characterized by a 40,000 K Maxwell-Boltzmann velocity distribution with a source strength of $1.9 \times 10^{28}$ H atoms $s^{-1}$.

**Figure 3. Comparison of Model Calculated and Observed Lyman-α Brightness for a Titan and Interior Source.** The observed preencounter Lyman-α brightness of hydrogen for a dawn to dusk approximately radial scan as measured by the Voyager 1 spacecraft in 1980 between day of year (DOY) 239 and 256 and presented by Shemansky and Hall (1992) is compared to a model calculation (solid line) including both a Titan source and an interior source. The Titan and the interior sources are the same as in Figure 1 except that their source strength are slightly reduced to $3.3 \times 10^{27}$ H atoms $s^{-1}$ and $1.4 \times 10^{28}$ H atoms $s^{-1}$, respectively.

**Figure 4. Comparison of Model Calculated and Observed Lyman-α Brightness for a Titan and Interior Source.** The model calculated mosaic image for the postencounter Lyman-α brightness of hydrogen measured by the Voyager 1 spacecraft in 1980 between day of year (DOY) 324 and 343 and presented by Shemansky and Hall (1992) is shown as a (relative brightness) contour plot for the same combined Titan and interior sources as in Figure 3. The filled circle in the center is Saturn to scale, and the dotted line is Titan's orbit projected unto the plane of view of the spacecraft with the line of sight intersecting the satellite orbit plane at an angle of about 26° looking down on the north pole.

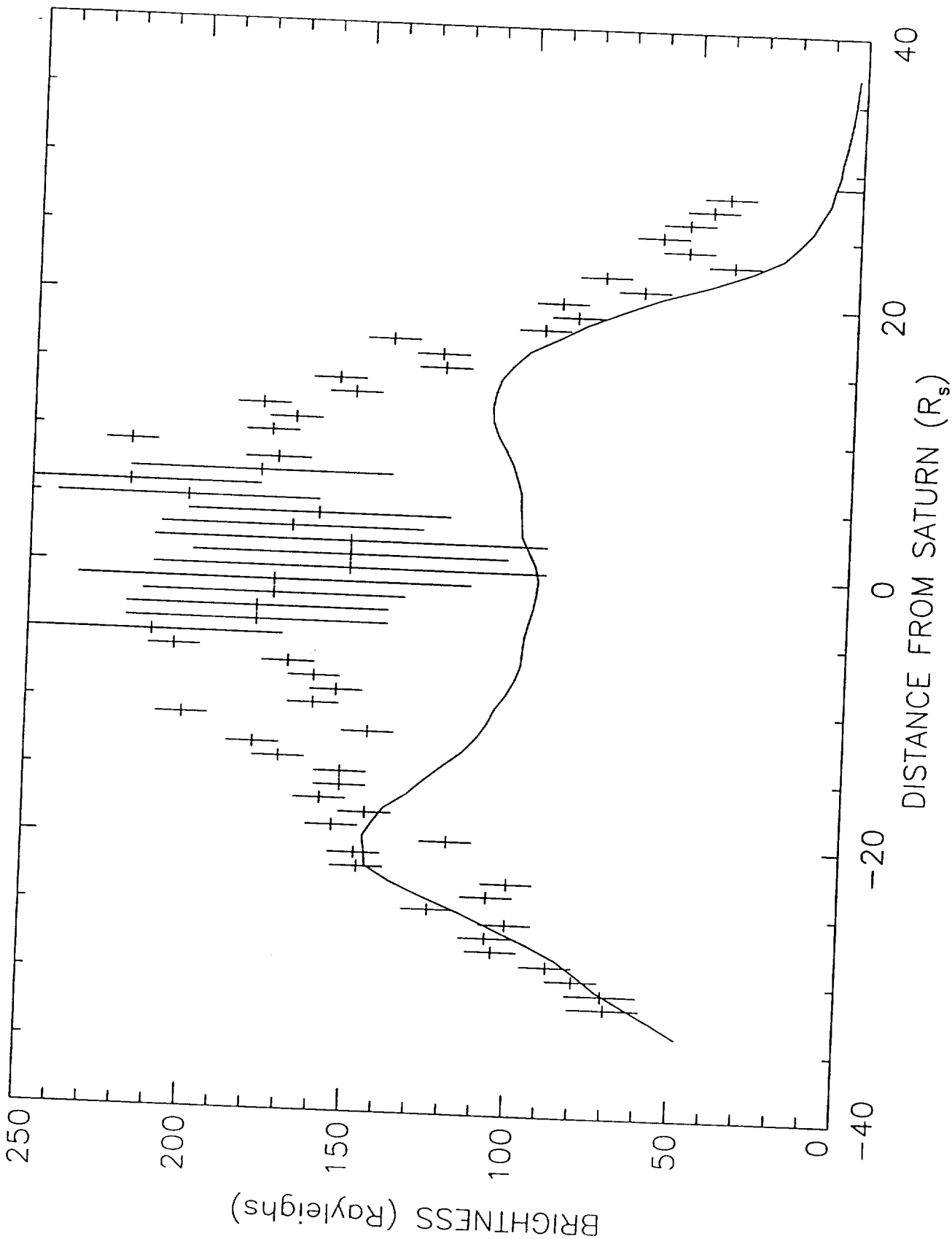
BRIGHTNESS (Rayleighs)
250
200
150
100
50
0
-40
-20
0
20
40
DISTANCE FROM SATURN ($R_s$)

Figure 1

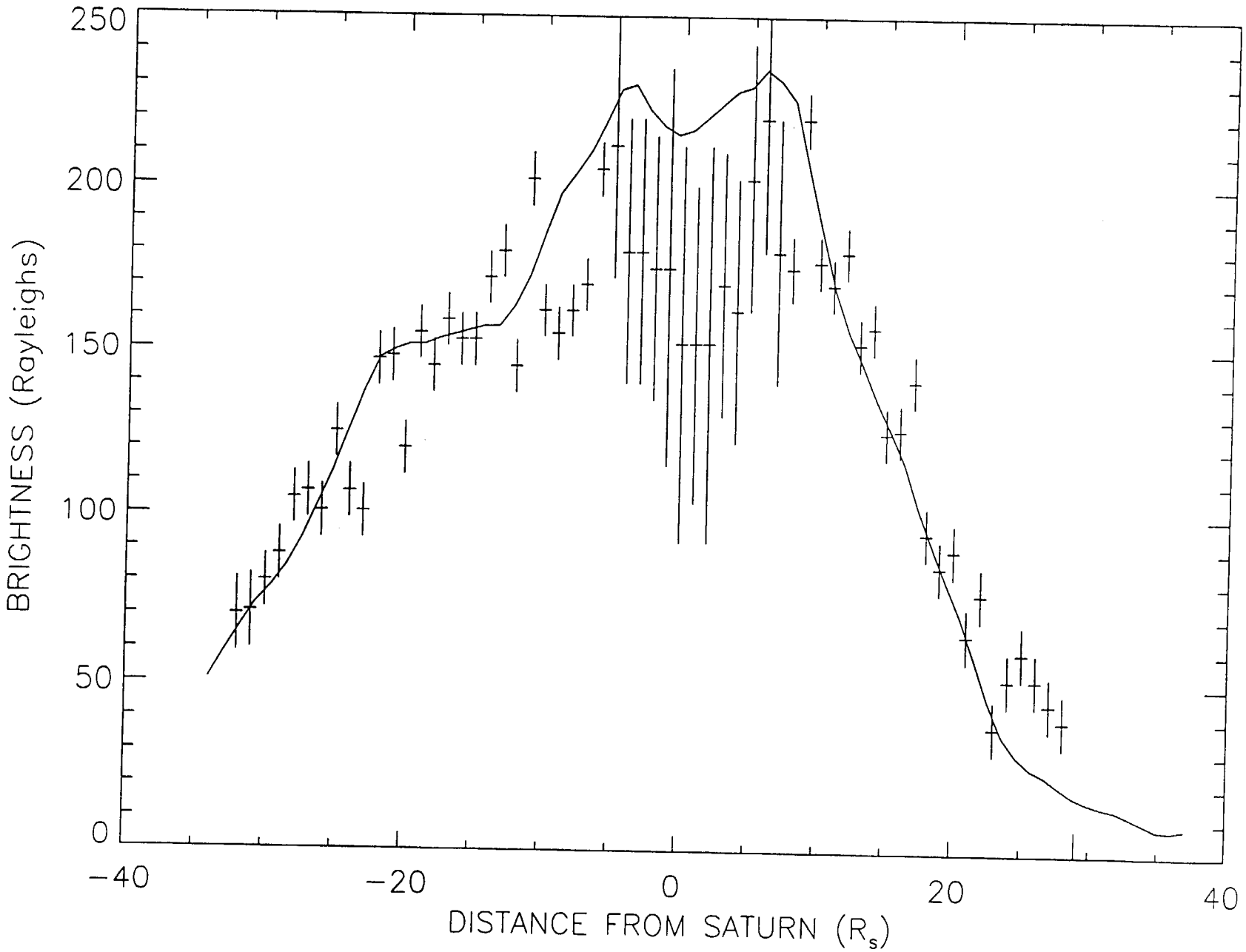
250
200
150
100
50
0
BRIGHTNESS (Rayleighs)
−40
−20
0
20
40
DISTANCE FROM SATURN ($R_s$)

Figure 2

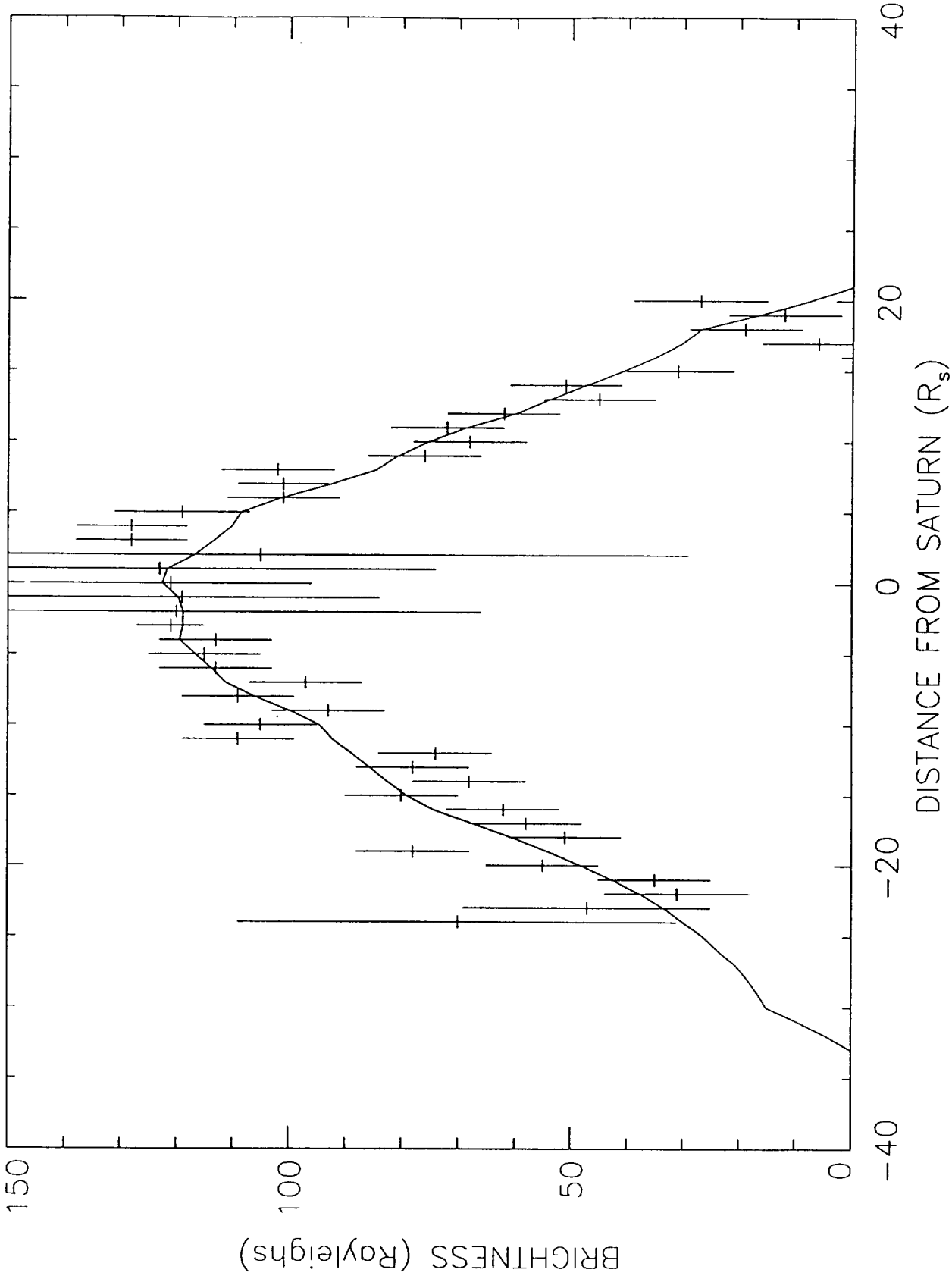
BRIGHTNESS (Rayleighs)
150
100
50
0
-40
-20
0
20
40
DISTANCE FROM SATURN ($R_s$)

Figure 3

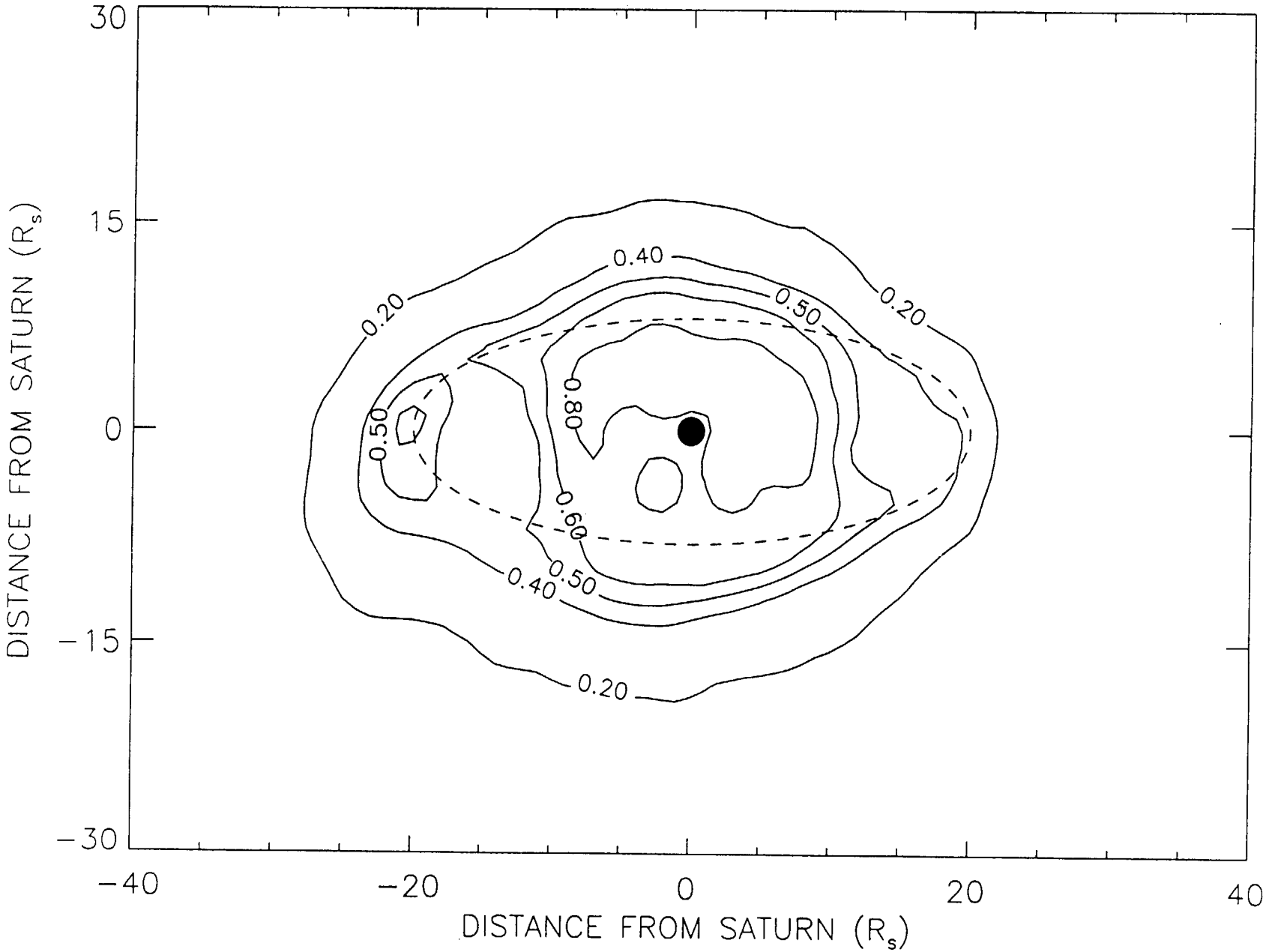
30
15
0
−15
−30
−40
−20
0
20
40
DISTANCE FROM SATURN ($R_s$)
DISTANCE FROM SATURN ($R_s$)
0.20
0.40
0.50
0.20
0.80
0.50
0.60
0.40
0.50
0.20

Figure 4

# APPENDIX

## A Study of Hydrogen in the Saturnian System

# A STUDY OF HYDROGEN IN THE SATURNIAN SYSTEM

M. L. Marconi
and
William H. Smyth

Submitted to
The Astrophysical Journal
July 23, 1997

Atmospheric and Environmental Research, Inc.
840 Memorial Drive
Cambridge, MA 02139

ABSTRACT

The existence of atomic hydrogen in the Saturnian system has been known for almost a quarter century. Despite extensive observation and modeling over this period of time, the spatial morphology and kinetic nature of the circumplanetary hydrogen are still not well understood. The reasons for this lack of understanding are that the basic physical nature of the sources of hydrogen are poorly characterized and that the only detailed spatial measurements of hydrogen are from the Voyager excursions through the system. In this study, we combine the numerically efficient approach discussed in Smyth and Marconi (1993) for the calculation of orbits with the Saturnian plasma model of Richardson (1995) to model the Voyager 1 and 2 UVS observations as presented by Shemansky and Hall (1992). Although the comparison is limited by the quality of the data, source rates for a Titanogenic source of $3.3 - 4.8 \times 10^{27}$ H atoms-$s^{-1}$ and, for the first time, source rates larger by about a factor of four for an interior source of hydrogen of $1.4 - 1.9 \times 10^{28}$ H atoms-$s^{-1}$ are obtained. These source rates for Titanogenic hydrogen are consistent with previous estimates. The source rates for the interior sources are consistent with recent estimates of source rates for other water group species based on observational consideration but are substantially higher than source strengths based on sputtering rate estimates. In addition to these source rates, some broad constraints on the energy and spatial distribution of hydrogen in the Saturnian system are also given.

# 1. INTRODUCTION

The existence of atomic hydrogen in the Saturn system was first predicted by McDonough and Brice (1973). Two years later, in 1975, rocket borne observations of Lyman-α emissions from near Saturn's rings (Weiser et al. 1977) detected atomic hydrogen for the first time. In 1976 and 1977, the earth-orbiting Copernicus satellite (Barker et al. 1980) provided evidence for hydrogen near Titan, in 1979 the Pioneer 11 spacecraft found hydrogen near Titan's location on its orbit and near the rings (Judge et al. 1980), and from 1978 to 1990 (McGrath and Clarke 1992), the International Ultraviolet Explorer (IUE) has been utilized at least once per year to observe the hydrogen near Saturn's disk. The most spatially detailed observations of hydrogen in the Saturnian system, however, remain those of the Voyager 1 and 2 missions that flew through the Saturn system in 1980 and 1981. These observations provided one-dimensional scans of the Lyman-α emissions from hydrogen throughout the entire Saturnian system (Broadfoot et al. 1981, Sandel et al. 1982) and also provided a detailed picture of the magnetospheric plasma (Bridge et al. 1981, 1982; Richardson and Sittler 1990) which is a critical component in understanding the sources and sinks for this hydrogen cloud distribution. As a result, most studies to date have focused upon the Voyager data in their attempts to explain the source and structure of this hydrogen.

In conjunction with the foregoing observational efforts, there has been substantial attention directed to a theoretical understanding of hydrogen in the

Saturnian System. The earliest studies (McDonough and Brice 1973 and Fang et al. 1976, for example) assumed that the only source of hydrogen was Titan, that the hydrogen was collisionless, that the only force acting on the hydrogen atoms was Saturn's gravity, and that the loss rate of hydrogen was, moreover, characterized by a single spatially homogeneous lifetime. Studies of Dennefeld (1974) considered a planetary source, a ring source, and a Titan source and concluded that the Saturn source was not significant, that an $H_2O$ atmosphere would exist for the rings, and that an H and $H_2$ torus would exist for Titan. For a Titan source, Smyth (1981) also included the effect of the gravity of Titan on the hydrogen atom orbits and calculated in three-dimensions the time evolution of the torus, showing that the circumplanetary hydrogen distribution for an appropriate H lifetime was essentially azimuthally symmetric with a density maximum near Titan's orbit. Generally speaking, these models led to a torus of hydrogen about Titan's orbit which was approximately axisymmetric (doughnut shaped), devoid of significant density inside of ~8 planetary radii, and whose density was determined by the source rate and assumed lifetime. This picture was broadly confirmed by the preliminary analysis of Broadfoot et al. (1981, 1982) of some of the Voyager 1 and 2 ultraviolet spectrometer (UVS) observations. Their analysis concluded that the hydrogen in the Saturnian system formed a roughly uniform torus, extending from 8 to 25 $R_S$ (Saturn radii), with a cavity within 8 $R_S$, and a typical density of 20 $cm^{-3}$. Although a post-Voyager model of the Titan H torus by Ip (1985) incorporated a one-dimensional (radial) lifetime profile, this picture of the hydrogen cloud dominated the general view until Shemansky and Hall (1992) analysed previously unpublished UVS observations and clearly

demonstrated that the hydrogen extended to Saturn and was characterized by a complex three dimensional structure quite unlike a doughnut. With this new asymmetric hydrogen cloud in mind, Smyth and Marconi (1993) studied the particle orbits of H atoms emanating from Titan. They introduced two new ingredients, namely, radiation pressure and the leading non-spherical component, $J_2$, to Saturn's gravity. While they did not specifically calculate the hydrogen cloud, they noted that the orbits obtained in this scenario would lead to a highly asymmetric cloud extending to Saturn. Ip (1995) explicitly calculated the hydrogen cloud produced by a Titan source for the scenario in Smyth and Marconi and confirmed that the cloud was quite asymmetric and extended as far in as Saturn. Ip also compared the radial density profile of the cloud to the UVS data presented by Shemansky and Hall and concluded that another source of hydrogen was necessary within 15 $R_S$.

Over the same period, other studies suggested that Titan was not the only source of atomic hydrogen in the Saturnian System. Shemansky et al. (1985) analysed Voyager 2 data and showed that atomic hydrogen extended into Saturn's atmosphere and Hilton and Hunten (1988) applied their model for hydrogen to the Voyager measurements and concluded that in order to explain the vertical extent of the hydrogen, Saturn must be the principal source of atomic hydrogen within 10 $R_S$. Further indirect support and a mechanism for Saturn as a major source of atomic hydrogen came from the Lyman-$\alpha$ dayglow phenomena observed at Saturn. Failure to account for the dayside Lyman-$\alpha$ dayglow by scattering of solar Lyman-$\alpha$ radiation led to the suggestion that collisional excitation of atomic

hydrogen by electrons in the upper atmosphere of Saturn (electroglow) could account for the excess Lyman-α brightness of Saturn (Shemanksy and Ajello 1983, Shemansky 1985, Shemansky et al. 1985, and Yelle et al. 1986). Furthermore, these electrons could produce, by impact dissociating $H_2$, enough sufficiently energetic hydrogen atoms to account for the atomic hydrogen cloud within ~8 $R_s$. Recently, however, Emerich et al. (1993) applied a new and improved radiative transfer model for the scattering of solar Lyman-α by H to various Lyman-α airglow data for the giant planets and concluded that the need for the electroglow process was much reduced. Ben Jaffel et al. (1995), using the same approach in a new analysis of the Voyager UVS H Lyman-α emission from Saturn, concluded that reflected Lyman-α was the main contributor to the brightness rather than collisional excitation. Hence, a mechanism for dispersing hydrogen atoms from Saturn to large distances is not presently clear.

The Voyager 1 and 2 plasma observations (Bridge et al. 1981, 1982) also focused attention on the surfaces in the Saturnian system as additional sources of atomic hydrogen. The rings of Saturn (Ip 1984) and icy surfaces of the Saturnian satellites, as a result of bombardment by magnetospheric plasma, solar radiation, and micrometeoroids, could directly generate atomic hydrogen or other heavier neutral species (Cheng et al. 1982, and Lanzerotti et al. 1983). Furthermore, gas phase chemical interactions between the heavier species, such as $H_2O$, with the plasma and solar radiation were also recognized as another source of atomic hydrogen. Chemical "one box" models of the magnetospheric ions and neutrals were constructed by Richardson et al. (1986) and Richardson and Eviatar (1987)

who concluded that the neutral density had to be quite small and supported the view that Titan was the major source of hydrogen in the Saturn magnetosphere. Johnson et al. (1989) calculated the spatial distribution of plasma sputtered $H_2O$ from the icy Saturnian satellites and found high density neutral tori associated with the satellites. Shemansky and Hall (1992) using a one box chemical model of the ions and neutrals in the Saturnian magnetosphere, which included some key chemistry neglected in the Richardson models as well as a more reasonable estimate of the ion diffusion rate, concluded that the neutral densities were much greater than the Richardson models predicted. The high density of neutrals in the Saturnian magnetosphere was recently confirmed by the Hubble space telescope's faint spectrograph observation of the OH radical near the orbit of Thetys (Shemansky et al. 1993). The large abundance of OH inferred from this observation created a problem in that the estimates of neutral production rates from icy satellite sputtering, as calculated by Johnson et al. 1989 for example, were well below the level required to sustain it. Shi et al. (1995) used new, substantially larger, sputtering rates derived from some recent laboratory measurements to determine the sputtering rates of neutrals from the icy satellites. While the rates were considerably higher, they still fell quite short of explaining the OH observation. Most recently, further observations by Hall et al. (1996) with the Hubble Space Telescope detected in addition large amounts of OH above the A and B rings of Saturn.

To summarize, it seems that there is general agreement that Titan is a substantial source of hydrogen for the Saturn magnetosphere. This hydrogen

probably dominates beyond roughly 10 $R_s$ and is generated at a rate roughly in the range of 2-5x$10^{27}$ atoms-$s^{-1}$. In the inner magnetosphere, however, other sources are dominant. The nature and strength of these sources are far less certain. Saturn's atmosphere would seem to have an abundance of hydrogen to supply to the inner magnetosphere. It is not clear, however, that the electroglow process is able to provide the requisite flux of hydrogen and, moreover, the recent reanalysis, mentioned above, of dayglow observations do not require a significant electroglow contribution to the Saturnian Lyman-$\alpha$ brightness in any case. The icy satellites and rings are sputtering sources of neutrals for the magnetosphere of Saturn. In this case, there is little problem with populating the inner magnetosphere with hydrogen atoms either directly or from the destruction of hydrogen bearing species such as $H_2O$. Up to the present, however, the sputtering source rates required to explain the neutral observations are substantially above the sputtering rates based on laboratory data.

The purpose of this paper is to address the nature and strength of the Saturn ring, icy satellite, and Titan sources of hydrogen in the Saturnian magnetosphere. A model which includes a Titan source, a Saturn source, and a source in the icy satellite region and ring region between Saturn and Titan (i.e., an interior source) is utilized to obtain source rates and some general characteristics of the interior sources by using Voyager observations of the hydrogen distribution enveloping the Saturnian system.

## 2. MODEL

The basic model that is used in this work essentially computes the density and brightness distribution of hydrogen emitted from a source under the assumption that the hydrogen is to a good approximation collisionless (Smyth and Marconi 1993). Following Smyth and Marconi (1993), the model includes Saturn's gravity, including the leading nonspherical, $J_2$ component, solar radiation pressure, loss of hydrogen atoms to reactions with magnetospheric and solar wind plasma, and collisional loss of hydrogen to Saturn and its rings. There are three basic steps to performing the model calculations presented below: (1) choosing the initial conditions for H atoms to be emitted, (2) calculating the orbits corresponding to these initial conditions, and (3) calculating orbital information so that spatial hydrogen densities and brightnesses may be determined.

### 2.1 INITIAL CONDITIONS

The first step in the model is to choose the initial velocities, positions, and emission times for the collection of hydrogen atoms, typically a hundred thousand, emitted from one of the three sources considered here, i.e. Titan, Saturn, or some interior source placed between Titan and Saturn. This process basically involves choosing the speed randomly from some speed distribution, for example Maxwellian, and the direction according to some angular distribution for the emission of a hydrogen atom. While various speed distributions were considered, the angular distribution was always taken as isotropic. In the case of Titan, the initial velocity distribution was based on an exospheric temperature of 186 K and

an exobase radius of 4175 km (Table 1). Assuming an isotropic Maxwellian with a temperature of 186 K at the exobase, the resulting velocity distribution at the Lagrange radius was approximated by reducing the energy of the particle by an amount equal to the gravitational potential energy between the exobase and Lagrange radius. A separate three body (including the gravity of Saturn and Titan) more exact calculation for the orbits between the exosphere and Lagrange radius of Titan, assuming a 186 K Maxwellian at the exobase of Titan, was also performed and confirmed that the simple reduction in energy yields a good approximation to the actual velocity distribution at the Lagrange radius for this case. The Titan source was then treated as a point in these calculations and the point of emission was the position of Titan in its orbit. Emission times were chosen at random over a time interval chosen sufficiently long so that initial transients would decay ($\sim 5 \times 10^7$ s). This was well satisfied for the chosen emission time interval of $2 \times 10^8$ s for particles emanating from Titan.

The interior source was treated almost identically to Titan. It was also taken in the planetary equator plane as a point source moving in a circular orbit around Saturn. The radial position of the source was varied between 2 $R_s$ and 15 $R_s$, however. In addition, the initial speed distributions of the emitted hydrogen, which included Maxwellians and modified sputtering distributions (Smyth and Combi 1988), were varied in contrast to the 186 K Maxwellian always assumed for Titan.

Finally, Saturn was treated as a source with radius, spin rate, and obliquity given in Table 1. The Saturn source was assumed to be emitting preferentially from the sunward hemisphere as suggested by observations (Shemansky and Hall 1992, for example). The source strength dependence on location on the sunward hemisphere was assumed uniform due to the lack of any position dependent information and also due to a lack of sensitivity of the results to the spatial dependence of the hydrogen source. The initial hydrogen speed distributions were, as for the interior source, varied. Since satellite orbits are difficult to populate (Hilton and Hunten 1988) only escape and ballistic orbits were considered. The effect of the rings was ignored since only a small fraction of orbits intersect the rings. Moreover, of the small fraction that strikes the rings, much of that will be scattered back towards Saturn which fills a large part of the sky as seen from the rings.

## 2.2 ORBIT CALCULATION

Once the initial velocity, position, and time of emission are determined, as described above, the orbit integration is performed. In this work, rather than following the spatial position of the atoms by directly time integrating the equations of motion, the initial conditions are converted into orbital elements and the evolution of the orbital elements in time are integrated as in Smyth and Marconi (1993). This approach accounts for the perturbative effects due to both the $J_2$ component of gravity and radiation pressure (values give in Table 1) which were shown to be important by Smyth and Marconi (1993). The advantage over the conventional approach of solving directly Newton's equations for the orbits is

that the integration proceeds much more quickly and, thus, permits a much larger number of particles to be used and many more scenarios to be tested.

## 2.3 DETERMINATION OF DENSITIES AND BRIGHTNESSES

In order to determine the hydrogen density or brightness, the loss of hydrogen must be calculated as the atoms travel along their orbits. As mentioned above, the model accounts for the loss of hydrogen from reactions with the magnetospheric and solar wind plasmas, collisions with Saturn and its rings, and escape of sufficiently energetic hydrogens from the system.

The model of the Saturnian magnetosphere used in this study is that of Richardson and Sittler (1990) and Richardson (1995). The equatorial densities, temperatures, and velocities, of the heavy ions, protons, hot electrons, and cold electrons from L shell, L = 1 to L = 20, were taken from Richardson (1995). These quantities were then used with Richardson and Sittler's (1990) model of force balance along the magnetic field line to generate the plasma properties above and below the equator plane. This field of plasma properties was converted into a field of loss rates (see Figure 1) which include charge exchange with the heavy ions, assumed to be $O^+$, charge exchange with protons, as well as impact ionization by the hot and cold electrons. Richardson (1995) provides two alternative models for the equatorial plasma properties between L = 12 and L = 20. Since model calculations turned out to be similar in both cases, only one (Richardson's alternative 1) of these alternative models is used in the computations below and in Figure 1.

The plasma information used here is derived from the Voyager plasma science instrument (PLS) and is restricted to an energy/charge range of 10 to 5950 Volts (Richardson and Sittler, 1990). As a result, the true loss rates should be higher since there is plasma with energy outside of the PLS energy window. The amount of plasma flux outside of the PLS window should be small, however, judging by the flat flux energy spectra toward the low energy limit of PLS, the rapid drop toward the high energy limit of PLS, and the much lower value of plasma fluxes measured by the Voyager low energy charged particle instrument (LECP) starting at ~100 keV (Shi et al. 1995). As a result, the magnetospheric plasma loss rate of hydrogen from plasma within the PLS energy window is probably a good approximation to the total loss rate unless there are unexpectedly large plasma fluxes at the unviewed energies.

Outside of the spatial range of the above PLS data, i.e. magnetic flux shell L = 20, the loss rate of hydrogen was assumed to be due to resonant charge exchange with solar wind protons and a nominal value of $2 \times 10^{-8}$ $s^{-1}$ was most often employed. This choice for the loss rate is similar to theoretical estimates of the rate assuming nominal solar wind parameters at earth of 6 protons $cm^{-3}$, a velocity of 400 km-$s^{-1}$, a charge exchange cross-section (Stebbings et al. 1964) of $7.5 \times 10^{-15}$ $cm^{-2}$, and then scaling to Saturn's heliocentric distance. This is also similar to the rate used by Ip (1995) of $3 \times 10^{-8}$ $s^{-1}$ beyond 25 $R_s$. Some models were also constructed for different values of the loss rate. The best agreement with data was, however, obtained for a loss rate near $2 \times 10^{-8}$ $s^{-1}$.

Because, for example, of the changing location of the solar wind bow shock, the plasma beyond 20 $R_s$ (Bridge at al. 1981, 1982) is quite variable in space and time so that it is difficult to accurately construct a suitable representation of the plasma which could be utilized in this model. It appears, however, that a broad spatial and temporal average of the measured plasma properties leads to a loss rate of the order of $10^{-8}$ $s^{-1}$. Moreover, the large spatial extent and long lifetime of the orbits penetrating this region means that only the average properties of the plasma are important rather than the smaller scale spatial and faster temporal plasma variations. Consequently, the choice of a spatially and temporally uniform loss rate with the above value is well justified. For all orbits, the relatively small contribution of solar photoionization of the hydrogen with a rate of $7.26 \times 10^{-10}$ $s^{-1}$ (Huebner et al. 1992) was also included.

The actual determination of the amount of hydrogen lost from reactions with the plasma is performed in three steps. In the first step, the orbital elements at the start of some integration time step are used to calculate the spatial location of the corresponding Kepler orbit. The orbit is then divided into a large number of uniform time intervals and the location of each time interval in space is computed. The small loss of hydrogen in each of these time intervals is determined with the loss rate model discussed above and then summed over each time interval to give a total loss for the orbit. In the second step, the total loss over an integration time step is calculated. The orbital elements are assumed to be unchanged over an integration time step so that the same Kepler orbit may be used. The total loss

over this integration timestep is then obtained by suitably scaling the orbital period with the ratio of integration timestep to the period of the Kepler orbit. In the third step, this loss is added to the amount of hydrogen present at the end of the previous time step and the procedure restarted with new updated orbital elements appropriate to the time corresponding to the start of the next integration time step.

Additional losses of hydrogen occur due to collisions with Saturn and its rings. Collisions with Saturn are instantly evident, when in the course of integrating the orbital elements, the eccentricity of the orbit becomes sufficiently close to 1. In this case, the particle is assumed to be absorbed by Saturn. In the event that the orbit of a particle intersects the rings of Saturn, the procedure followed is similar to Ip (1995), i.e. if a particle crosses the equator within 2.27 $R_s$ the probability of absorption is 0.26 corresponding to an optical depth of 0.3. Since the results are not particularly sensitive to the presence of rings, this simple model of ring absorption is sufficient for this study. Finally, if the atom is on an escape orbit, the orbit is tracked to some distance slightly greater than the region of interest ($\pm 40$ $R_s$ from Saturn) and then the atom is assumed lost.

In order to calculate density and Lyman-$\alpha$ brightness, a three-dimensional grid is overlaid on the collection of orbits generated in the orbit integration part of the model described above. The grid used in this study consists of 80 x 80 x 60 boxes in the x, y, and z directions of size 1 $R_s$ x 1 $R_s$ x 1 $R_s$ respectively. The spatial coordinates (x,y,z) were chosen to define an inertial coordinate system centered at

Saturn with x and y in the equatorial plane and z perpendicular. The hydrogen density in this grid is determined by recording whether an orbit traverses a particular box and then correcting for the fraction of hydrogen remaining at that point due to lifetime processing. The contribution per unit volume to the brightness, i.e. the amount of solar Lyman-$\alpha$ resonantly scattered, is determined by multiplying the density by a g-factor which accounts for the heliocentric distance of Saturn and relative velocity of the atom and the Sun. This is similar to Smyth et al. (1995) except that the g-factor used here was normalized to the time dependent solar Lyman-$\alpha$ flux averaged over the observation period and scaled to Saturn's heliocentric distance (Hall 1997 and Pryor 1997). The contributions per unit volume to the brightnesses in the grid boxes, described above, are summed along the appropriate line of sights and convolved with the appropriate Voyager slits, given in Shemansky and Hall (1992), to finally obtain the brightnesses for the images and radial profiles shown below.

Before we proceed to a presentation of the results of this study, there are two items which should be mentioned. The first is that impinging on the Saturnian system there is a flow of interstellar hydrogen which could effect the distribution of hydrogen emanating from the sources of hydrogen in the Saturnian system. Using nominal values from Allen (1976) of a density of 0.1 $cm^{-3}$ and velocity of 21 $km\text{-}s^{-1}$ for the interstellar hydrogen, the collision rate with the Saturnian system hydrogen is of the same order of size as the photoionization rate, i.e. $10^{-9}$ $s^{-1}$. This may be neglected in comparison to the smallest rate in our plasma loss rate model of $2x10^{-8}$ $s^{-1}$ for hydrogen in the solar wind plasma.

Another potentially important issue regards the neglect of the effect of Titan on the hydrogen orbits. A hydrogen wandering sufficiently close to Titan could be captured or strongly scattered. If we assume that this "sweeping" radius of Titan is equal to its Lagrange radius, ~20 Titan radii ($R_T$) (Table I), then model computations of the amount of hydrogen in the neighborhood of Titan's orbital location indicate that if it is assumed that this hydrogen is stationary in the Saturnian inertial frame, Titan's Lagrange sphere would intercept an amount of hydrogen equivalent to roughly an amount comparable to the hydrogen emanating from Titan. This would have significant consequences for the hydrogen cloud. In reality, however, most hydrogen atoms have sufficient velocity relative to Titan so that they would have to penetrate to well within the Lagrange sphere before being substantially perturbed by Titan's gravity. If we assume that the mean speed, relative to Titan, of a hydrogen atom in the neighborhood of Titan's orbit is about the same as the mean speed of the initial distribution of hydrogen atoms from Titan at the Lagrange radius of ~1.4 km-$s^{-1}$, then a hydrogen atom would have to penetrate to ~4 to 6 $R_T$ from Titan before being significantly disturbed by Titan's gravity. Therefore, it is likely that the effective sweeping rate of Titan is a small fraction of the production rate of hydrogen from Titan and the neglect of Titan's gravity in this work is justified.

## 3. RESULTS

Figure 2 is a comparison of the Lyman-$\alpha$ model brightness (solid line) of the hydrogen cloud due to a purely Titanogenic source of $4.8 \times 10^{27}$ atoms $s^{-1}$ with the observed brightness (crosses) obtained by accumulating the Voyager 2 UVS approximately radial scans taken from day of year (DOY) 180 to DOY 186 in 1981 as described in Shemansky and Hall (1992). The brightness asymmetry in the double-peaked model profile is produced by the action of solar radiation acceleration. Clearly, the match is inadequate and strongly suggests that an additional, more centrally located source of hydrogen is required, as was also pointed out by Ip (1995).

In Figure 3, the same data is the subject of comparison. The model, however, now includes two sources. The same Titanogenic source that was used in Figure 2 is combined with an internal source of $1.9 \times 10^{28}$ atoms $s^{-1}$ at 8.7 $R_s$ which corresponds to Rhea's orbital position. This interior source is assumed to generate hydrogen atoms with a 40000 K Maxwellian. The matching of the model to the data displayed in Figure 3 is achieved by adjusting the ratio of the Titan to interior source contribution and overall normalization until the model brightness profile approximates some mean trajectory through the region defined by the data points and their error bars. The data profile displays significant oscillations which are not evident in the model. These oscillations, however, are largely spurious (Doyle, 1996) and a mean curve through the data is an appropriate basis for a comparison. In Figure 4, the same two sources are similarly adjusted with slightly

smaller source rates to match the nearly radial UVS scans accumulated to produce the H Lyman-α intensities obtained by Voyager I during the period DOY 239 to 256 in 1980 (Shemansky and Hall, 1992). For both sets of data, Figure 3 and Figure 4, the agreement of the model with the data is quite good and certainly is vastly improved over the case of the Titanogenic source alone shown in Figure 2.

The choice of the 40000 K Maxwellian for the interior hydrogen source represents the best of a large number of other models with different initial velocity distributions. A wide variety of other velocity distributions were tried which included other Maxwellians with different temperatures as well as various sputtering distributions. It was found that any distribution with a characteristic energy that was not too small, i.e. much below about 0.5 eV, could be combined with the canonical Titan source, described above, to produce a profile which was in reasonable agreement with the data shown in Figures 3 and 4. In addition, the source rates inferred for the other distributions were similar to those obtained for the 40000 K case. The actual source of H is likely to have a complex velocity distribution since there are various different sources for hydrogen. H may be generated from $H_2O$, OH, and $H_2$ as a result of photodissociation or electron impact dissociation. H may also be directly generated from surface sputtering. All these sources contribute H atoms with velocity distributions characteristic of the particular source. Moreover, since H is light, it will likely not be spatially localized near its source. As a result, the determination of the nature and distribution of the sources of H is not a straightforward task, particularly in view

of the limited sensitivity of the data considered here to the details of the velocity and source distribution for H.

In order to test the effect of the placement of the interior source, a number of models were constructed with the interior source placed at different locations ranging from 3 $R_s$ to 15 $R_s$. It was found that only if the source was in the neighborhood of 8 $R_s$, as in the interior model used in Figures 3 and 4, was a satisfactory match obtained. This, however, should not be interpreted as implying that the major source of hydrogen is in the neighborhood of Rhea's orbital location. As for the velocity distribution of hydrogen, there is limited sensitivity to the choice of source. The exact spatial distribution of the source is not well determined by the data model comparison displayed in Figures 3 and 4. The obtaining of a better match with an interior source at 8.7 $R_s$ actually only indicates that the source of non-Titanogenic hydrogen is largely confined to inside of around 8 or 9 $R_s$. The precise distribution of the source within that radial distance is not well determined in this comparison. Models with a Saturn source of H were also calculated with the result that Saturn is only a minor contributor at least outside of the immediate location of Saturn where the error bars in the data are rather large. This is consistent with the Lyman-$\alpha$ dayglow being due to scattering of Lyman-$\alpha$ radiation rather than collisional processes which could produce energetic hydrogen.

Numerical models were also computed with different loss rates for H in the solar wind plasma. A definite preference for a loss rate 1.5 - $2.0 \times 10^{-8}$ $s^{-1}$ (lifetime

$5x10^7$ s) was noted. Other choices of loss rates, significantly outside this range, yielded clearly inferior agreement with the data in Figures 3 and 4. It is interesting to note that this rate is very similar to the simple scaling to Saturn's heliocentric distance of the charge exchange rate for H near the Earth using nominal solar wind conditions.

Source rates for H obtained for Titan and the interior source were, respectively, for the data in Figure 3, $4.8x10^{27}$ atoms $s^{-1}$ and $1.9x10^{28}$ atoms $s^{-1}$, while for the data in Figure 4 were, respectively $3.3x10^{27}$ atoms $s^{-1}$ and $1.4x10^{28}$ atoms $s^{-1}$. In both cases the interior source is about 4 times larger than the Saturn source. This discrepancy (~40%) in the absolute source rates between the two dates could arise from a number of factors associated with the modeling such as the matching of the model to data which is an estimation by eye of a reasonable approximation to the highly oscillatory data. In addition, the slit geometry is complicated with only representative examples shown in Shemansky and Hall (1992). It also appears that the data processing performed by Shemansky and Hall is quite involved so that together with the modeling performed here, there is ample opportunity for spurious variations to enter the data model comparisons. In principle, since the measurements were well separated in time, intrinsic variation of the source could be also possibility. It is not clear why both sources, however, should be affected and in almost the same proportion. Another possibility is that the solar Lyman-$\alpha$ brightness information used in this study is based on the He 10830 proxy method rather than direct measurement of solar Lyman-$\alpha$ luminosity. Since the Lyman-$\alpha$ solar luminosity is known to vary by

as much as 40% over a solar cycle (Skinner et al. 1988), this represents another potential source for the differences in the inferred source rates for H.

The source rates derived for the Titan source are in the range of 2-5x$10^{27}$ atoms $s^{-1}$ which, as mentioned above, are in the generally expected range. The hydrogen source rates for the interior source correspond to an $H_2O$ source rate of 7-10x$10^{27}$ molecules $s^{-1}$ assuming H is mainly from $H_2O$ and OH (assuming OH is also mainly from $H_2O$). This is an order of magnitude higher than the maximum total sputtering rate given by Shi et al. (1995). According to Bar-Nun et al. (1985), however, comparable amounts of H, and $H_2O$ may be sputtered as well. If this is true, the actual amount of $H_2O$ required may be reduced by a factor of 2 or 3 to a few x $10^{27}$ molecules-$s^{-1}$ so that the discrepancy with the estimates of Shi et al. may be closer to a factor of 2 or 3. While Shi et al. have employed the latest laboratory data to estimate these rates, we repeat the comment by Shemansky and Hall (1992) that there is an inherent difficulty in translating laboratory surface reactions to icy satellite surfaces. In addition, there are other means of ejecting $H_2O$ molecules from the surfaces in this system, such as micrometeoroids, not treated in their work. The largest $H_2O$ production rate of 7-10x$10^{27}$ molecules $s^{-1}$ estimated above is, however, consistent with Shemansky and Hall (1992) who estimated a loss rate of O of 3x$10^{27}$ atoms-$s^{-1}$ within 4.5 $R_s$, if a comparable rate of loss occurs between 4.5 $R_s$ and the outer position of our interior source at about 9 $R_s$. It appears that larger rates of $H_2O$ production than can be accounted by Shi et al. are also implicated in the amount of OH detected by Shemansky et al. (1993) at 4.5 $R_s$ as well as the amount of OH reported near Saturn's rings by Hall et al.

(1996) as concluded by Ip (1997). In both cases, a factor of 2 or 3 more sputtering of $H_2O$ is required which is consistent with our findings if significant amounts of H and $H_2$ are also sputtered.

Figure 5 is a contour plot of the relative solar Lyman-$\alpha$ brightness corresponding to the observing geometry for the image displayed in Figure 1 of Shemansky and Hall, i.e. during the period 1980 DOY 324-343. The solid circle in the center is Saturn and the dotted line is Titan's orbit as would appear from Voyager's vantage point. The Sun is in the direction of the arrow. The same mixture of Titan source and interior source was used as in Figure 4. This comparison of the model with image is highly desirable as it would ordinarily represent a much more severe test of the validity of the model than the one dimensional data model comparisons discussed above. In this case, however, there appears to be substantial noise in the image. The only definite pattern evident is that both model and data are moderately brighter in the upper half of the ellipse defined by Titan's orbit (dotted line in Figure 5). It also appears that the overall magnitude of brightness variation is similar and that in both cases there appears to be a bright spot near the left hand apex of the orbit. Within the limitations of the data and the simplicity of the sources in the model it would appear that the model and data are broadly consistent.

The enhanced brightness in the region above Saturn in Figure 5 also suggests that the interior source is much stronger than the Titanogenic source. The orbital dynamics of an atom produced by gravity and radiation pressure leads to an

orbital evolution as shown in Figure 6 (see also Smyth and Marconi, 1993) which is for a typical Titanogenic hydrogen. In Figure 6 it is seen that there is an accumulation of material on the left of the Sun-planet line. A large fraction of this material is eventually lost by collisions with Saturn. Since the temperature of the Titanogenic source is relatively small, the hydrogen atoms from Titan tend to execute orbits with small eccentricities and thus avoid the high density plasma inside of Titan's orbit. As a result, the plasma lifetime of the Titanogenic hydrogens is comparable to the time required for an orbit to undergo the evolution depicted in Figure 6 which requires $\sim 10^8$ s. The result is an accumulation of material to the left of the sun planet line as implied in Figure 6. This Titanogenic hydrogen corresponds to below Saturn on Figure 5 and is contrary to what is observed. On the other hand, the orbits generated from the interior source are of high eccentricity due to the assumed high temperature of the interior relatively source and thus pass through the dense plasma where the hydrogen lifetime is short (Figure 1). While these orbits engage in the same evolution as depicted in Figure 6, they are more quickly destroyed by the plasma so that at any given time the distribution of surviving orbits have evolved for a time short compared to the evolution time. As a result, there will be more interior source hydrogen atom orbits to the right of the sun planet line since some of the orbits to the left will have been lost by collisions with Saturn. Thus, the interior source tends to produce a somewhat larger brightness above Saturn as seen in Figure 5. This supports the result obtained above that the interior source is substantially stronger (~ factor of 4) than the Titanogenic source. Indeed calculations with an

interior source strength not substantially greater than the Titan source strength failed to generate an enhanced brightness above Saturn.

## 4. CONCLUSIONS

A model for the distribution of hydrogen in the Saturn system was applied to the best published observational data of Shemansky and Hall (1992). While the model for the source of hydrogen could be made more complex, it seems that the H Lyman-α brightness data collected by Voyager 1 and 2 for the Saturn encounter, as presented in Shemansky and Hall (1992), does not permit a model data comparison which is particularly sensitive to either the detailed spatial location or energetics of the hydrogen interior source. This means that a more sophisticated model would not be likely more illuminating. There is, however, current work in progress to further reduce the Voyager observations (Herbert 1997), and it is anticipated that this will permit a more incisive model data comparison. Despite these limitations, it was possible to obtain very reasonable agreement between model and data which permitted a number of conclusions. Firstly, there is no question that a Titanogenic source alone is unable to account for the Lyman-α brightness data collected by Voyager. While a Titan source of $3.3 \times 10^{27}$ to $4.8 \times 10^{27}$ hydrogen atoms $s^{-1}$, consistent with previous estimates, was found to be necessary, an additional and larger by a factor of ~4 interior source of 1.4 to $1.9 \times 10^{28}$ hydrogen atoms-$s^{-1}$ was also required. This latter source implies a source rate of $H_2O$ large compared to estimates based on sputtering of the surfaces in the Saturnian system, but possibly consistent with recent measurements of

OH. The spatial location of the interior source was not well characterized except that it must start to become large in the neighborhood of about 9 $R_s$. The characteristic energy of the source hydrogens was also not well characterized except that the typical energy of the hydrogen from the interior source should not be much below about 0.5 eV. Possibly due to the large error bars in the data near Saturn, we were unable to detect any important source of hydrogen from Saturn. Finally, it also appears that an estimate of the time averaged lifetime of hydrogen in the solar wind plasma at Saturn's heliocentric position is $5\text{-}7 \times 10^7$ s.

ACKNOWLEDGEMENTS

We are grateful to Dr. F. Herbert and Dr. D. T. Hall for useful discussions. We also thank Dr. F. Herbert for providing us with SEDR data and solar Lyman-$\alpha$ brightness data and Dr. J. D. Richardson for providing us with his model for the Saturnian magnetospheric plasma.

REFERENCES

Allen, C. W. 1976, Astrophysical Quantities (London: William Clowes and Sons)

Barker, E., Cazes, S. Emerich, C. Vidal-Madjar, A., & Owen, T. 1980, ApJ, 242, 383

Bar-Nun, A., Herman, G. Rappaport, M. L., & Mekler, Y. 1985, Surface Science, 150, 143

Ben Jaffel L., Prange, R., Sandel, B. R., Yelle, R. V., Emerich, C., Feng, D., & Hall, D. T. 1995, Icarus, 113, 91

Bridge, H. S., Belcher, J. W., Lazarus, A. J., Olbert, S., Sullivan, J. D., Bagenal, F., & Gazis, P. R. 1981, Science, 212, 217

Bridge, H. S., Bagenal, F., Belcher, J. W., Lazarus, A.J., McNutt, R. L., Sullivan, J. D., & Gazis, P. R. 1982, Science, 215, 563.

Broadfoot, A. L., Sandel, B. R., Shemansky, D. E., Holberg, J. B., Smith, G. R., Strobel, D. F., McConnell, J. C., Kumar, S., Hunten, D. M., Atreya, S. K., Donahue, T. M., Moos, H. W., Bertaux, J. L., Blamont, J. E., Pomphrey, R. B., & Linick, S. 1981, Science, 212, 206

Burns, J. A. 1986, Some Background about Satellites, In Satellites ed, J. A. Burns and M. S. Matthews (Tucson: Univ. of Arizona Press)

Cheng, A. F., Lanzerotti, L. J., & Pironello, V. 1982, J. Geophys. Res., 87, 4567

Dennefeld, M. 1974, IAU Symposium 65, Exploration of the Planetary System, ed. A. Woszczyk and C. Iwaniszewska (Dordrecht: Reidel) 471

Emerich, C., Ben Jaffel, L., & Prange, R. 1993, Planet Space Sci, 41, 163

Fang, T.-M., Smyth, W. H., & McElroy, M. B. 1976, Planet. Space Sci. 24, 577

Hall, D. T. 1996, private communication.

Hall, D. T. 1997, private communication.

Hall, D. T., Feldman, P. D., Holberg, J. H., & McGrath, M. A. 1996, Science, 272, 516

Herbert, F. 1997, private communication.

Huebner, W. F., Keady, J. J., & Lyon, S. P. 1992, Ap&SS, 195, 1

Hunten, D. M., Tomasko, M. G., Flaser, F. M., Samuelson, R. E., Strobel, D. F., & Stevenson, D. J. 1984, Titan, Saturn, ed. T. Gehrels and M. S. Matthews (Tucson: Univ. of Arizona Press) 671

Ip, W. H. 1984, J. Geophys. Res., 89, 8843

Ip, W.-H. 1985, "The Atmosphere of Saturn and Titan", Workshop, Alpbach, Austria 16-19 September, ESP SP-241

Ip, W. H. 1995, ApJ, 457, 922

Ip, W. H. 1997, Icarus, 126, 42

Judge, D. L., Wu, F. M., & Carlson, R. W. 1980, Science, 207, 431

Lanzerotti, L. J., Brown, W. L., Johnson, R. E., Barton, L. A., Riemann, C. T., Garrrett, J. W., & Boring, J. W. 1983, J. Geophys. Res., 88, 8765

McDonough, T. R., & Brice, N. M. 1973, Icarus, 20, 136

McGrath, M. A., & Clarke, J. T. 1992, J. Geophys. Res., 97, 13691

Pryor, W. 1997, private communication.

Richardson, J. D. 1995, J. Geophys. Res., 22, 1177

Richardson, J. D. 1996, private communication.

Richardson, J. D., & Eviatar, A. 1987, Geophys. Res. Lett., 14, 999

Richardson, J. D., Eviatar, A., & Siscoe, G. L. 1986, J. Geophys. Res., 91, 8749

Richardson, J. D. & Sittler, E. C. 1990, J. Geophys. Res., 95, 12,019

Sandel, B. R., Shemansky, D. E., Broadfoot, A. L., Holberg, J. B., Smith, G. R., McConnell, J. C., Strobel, D. F., Atreya, S. K., Donahue, T. M., Moos, H. W., Hunten, D. M., Pomphrey, R. B., & Linick, S. 1982, Science 215, 548

Shemansky, D. E. 1985, J. Geophys. Res., 90, 2673

Shemansky, D. E., & Ajello, J. M. 1983, J. Geophys. Res., 88, 459

Shemansky, D. E., & Hall, D. T. 1992, J. Geophys. Res., 97, 4143

Shemansky, D. E., Matheson, P., Hall, D. T., Hu, H.-Y., & Tripp, T. M. 1993, Nature, 363, 329

Shemansky, D. E., Smith, G. R., & Hall, D. T. 1985, EOS Trans. AGU, 66, 1008

Shi, M., Baragiola, R. A., Grosjean, D. E., Johnson, R. E., Jurac, S., & Schou, J. 1995, J. Geophys. Res, 100, 26387

Skinner, T. E., Deland, M. T., Ballester, G. E., Coplin, K. A., Feldman, P. D., & Moos, H. W. 1988, J. Geophys. Res., 93, 29

Smyth, W. H. 1981, ApJ, 246, 345

Smyth, W. H., & Combi, M. R. 1988, ApJ, 328, 888

Smyth, W. H., & Marconi, M. L. 1993, Icarus, 101, 18

Smyth, W. H., Marconi, M. L., & Combi, M. R. 1995, Icarus, 113

Weiser, H., Vitz, R. C., & Moos, H. W. 1977, Science, 197, 755

Yelle, R. V., Sandel, B. R., Shemansky, D. E., & Kumar, S. 1986, J. Geophys. Res., 91, 8756

FIGURE LEGENDS

**Figure 1. Plasma Loss Rate For H.** The loss rate model of H, used in this study, from the plasma processes of charge exchange and electron impact ionization in the Saturnian magnetospheric plasma is contoured as a function of radial distance along Saturn's equatorial plane and vertical distance above it. The model is based on the Saturnian magnetospheric model of Richardson (1995, 1996) and Richardson and Sittler (1990). The contours are in units of $10^{-8}$ $s^{-1}$. The region between ~ 12 and 20 $R_s$ with contour values of $2x10^{-7}$ $s^{-1}$ actually contains an oscillatory lifetime structure with $2x10^{-7}$ $s^{-1}$ being roughly the size of the maxima.

**Figure 2. Comparison of Model and Data Brightness (Titanogenic Hydrogen only).** The Lyman-α brightness distribution corresponding to the Voyager 2 UVS scans conducted during the period 1981 DOY 180 to 186 (see Shemansky and Hall 1992) is shown. The crosses are the data and solid line is the model brightness distribution for a Titan source only with an H atom source rate of $4.8x10^{27}$ $s^{-1}$.

**Figure 3. Comparison of Model and Data Brightness For the Period 1981 DOY 180 to 186.** The Lyman-α brightness for the Voyager 2 scans for the period DOY 180 to 186 in 1981 are the crosses and the model is the solid curve which consists of a Titan source of $4.8x10^{27}$ atoms $s^{-1}$ and an interior source of $1.9x10^{28}$ atoms $s^{-1}$ at 8.7 $R_s$ with a 40000 K Maxwellian velocity distribution.

**Figure 4. Comparison of Model and Data Brightness For the Period 1980 DOY 239 to 256.** The Lyman-α brightness for Voyager 1 scans for the period DOY 239 to 256 in 1980 are the crosses while the solid line is the model brightness for a Titan source of $3.3 \times 10^{27}$ atoms $s^{-1}$ and an interior source of $1.4 \times 10^{28}$ atoms $s^{-1}$ with a 40000 K Maxwellian velocity distribution.

**Figure 5. Contour plot of Lyman-α Brightness.** The relative brightness of the same two source rates used in Figure 4 is contoured for the Voyager 1 observing geometry during the period 1980 DOY 324-343. The black dot in the center is Saturn and the dotted line is Titan's orbit. The brightness distribution has a general overall resemblance to the image in Shemansky and Hall (1992) and, in particular, is similarly somewhat brighter on the upper half. The Sun is to the right as shown by the arrow.

**Figure 6. Time Evolution of an H Atom Lost From Titan.** A typical orbit for an H atom from Titan is displayed at various times. The orbit which evolves under the action of radiation pressure and the $J_2$ component of Saturn's gravity undergoes an evolution characterized by a decrease in eccentricity and a rotation of the major axis of the orbit. The particle eventually crashes into Saturn after $\sim 10^8$ s. The star is towards the Sun and the numerals 2, 3, and 4 correspond to times of $3 \times 10^7$, $5 \times 10^7$, and $7 \times 10^7$ seconds respectively.

TABLE 1

Physical Parameters for Titan and Saturn

| | |
|---|---|
| Titan Exospheric Temperature (K) | 186 |
| Titan Radius (km) | 2575 |
| Titan Exobase Radius (km) | 4175 |
| Titan Lagrange Radius (km) | 52393 |
| Saturn Radius (equatorial) (km) | 60330 |
| Saturn Spin Rate (rad-sec$^{-1}$) | $1.662 \times 10^{-4}$ |
| Saturn Obliquity (deg) | 26.73 |
| $J_2$ | $1.6298 \times 10^{-2}$ |
| Radiation Acceleration (cm-sec$^{-2}$) | $6.29 \times 10^{-3}$ |

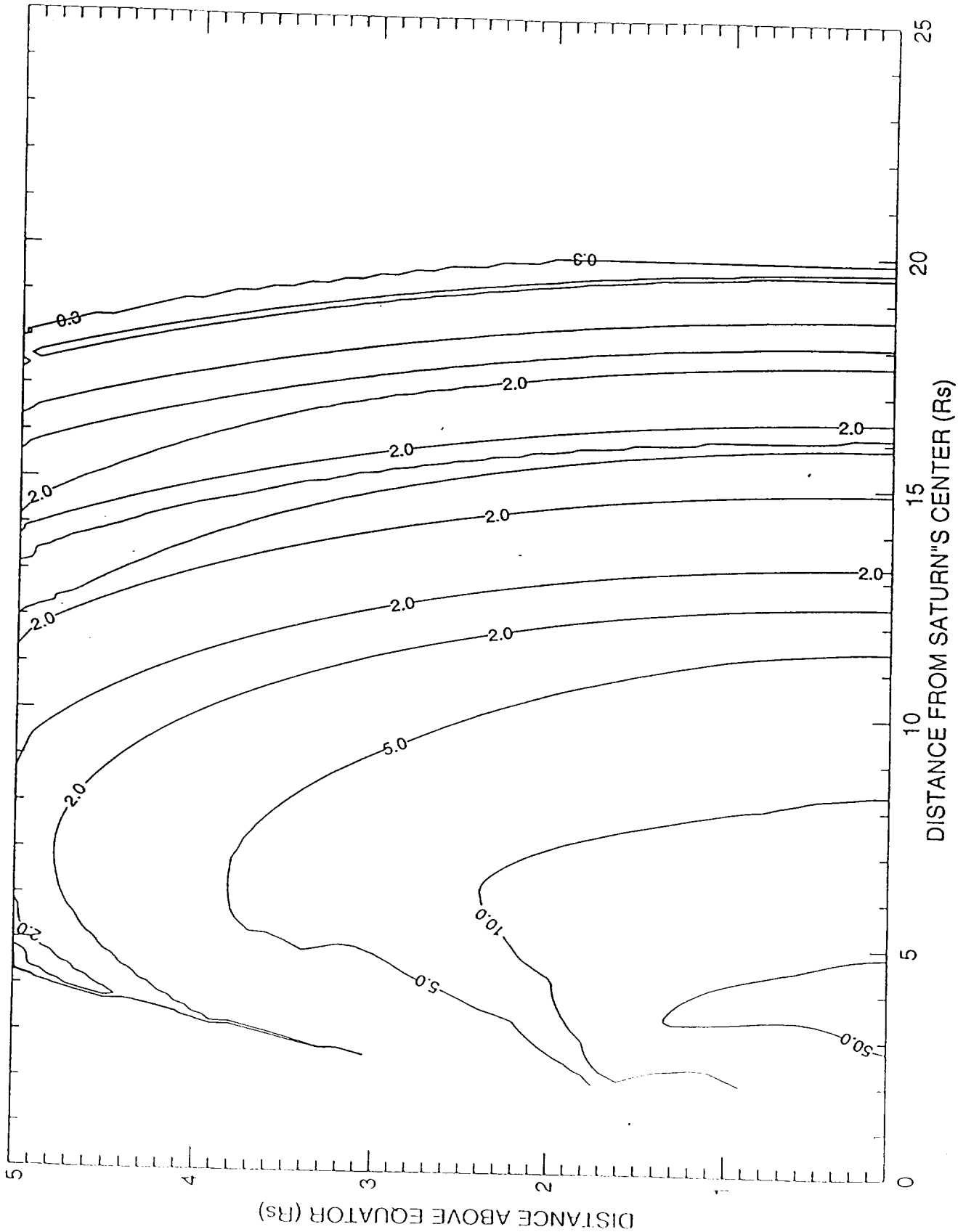
0.3
2.0
5.0
10.0
50.0
0
5
10
15
20
25
DISTANCE FROM SATURN'S CENTER (Rs)
0
1
2
3
4
5
DISTANCE ABOVE EQUATOR (Rs)

Figure 1

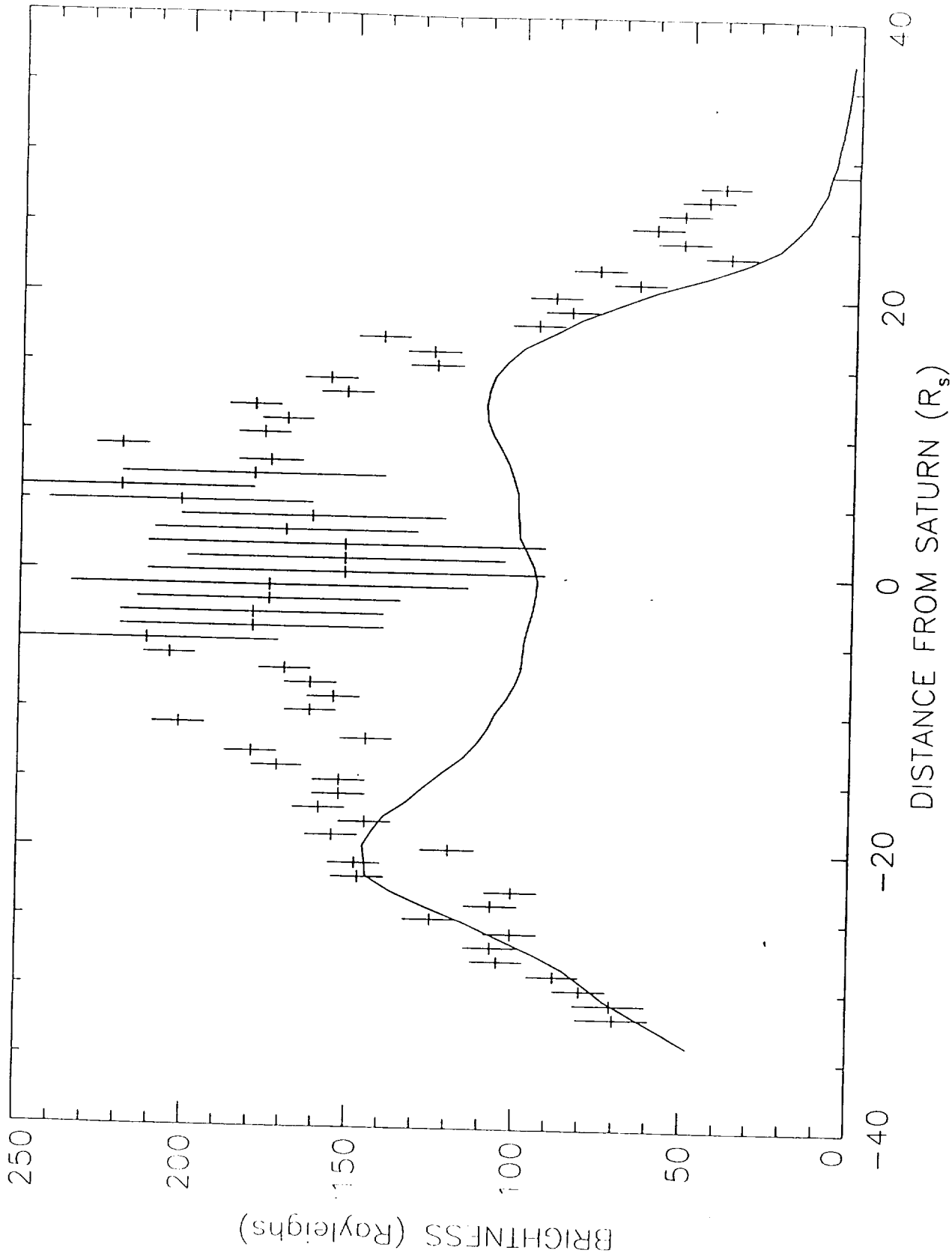
BRIGHTNESS (Rayleighs)
250
200
150
100
50
0
-40
-20
0
20
40
DISTANCE FROM SATURN ($R_s$)

Figure 2

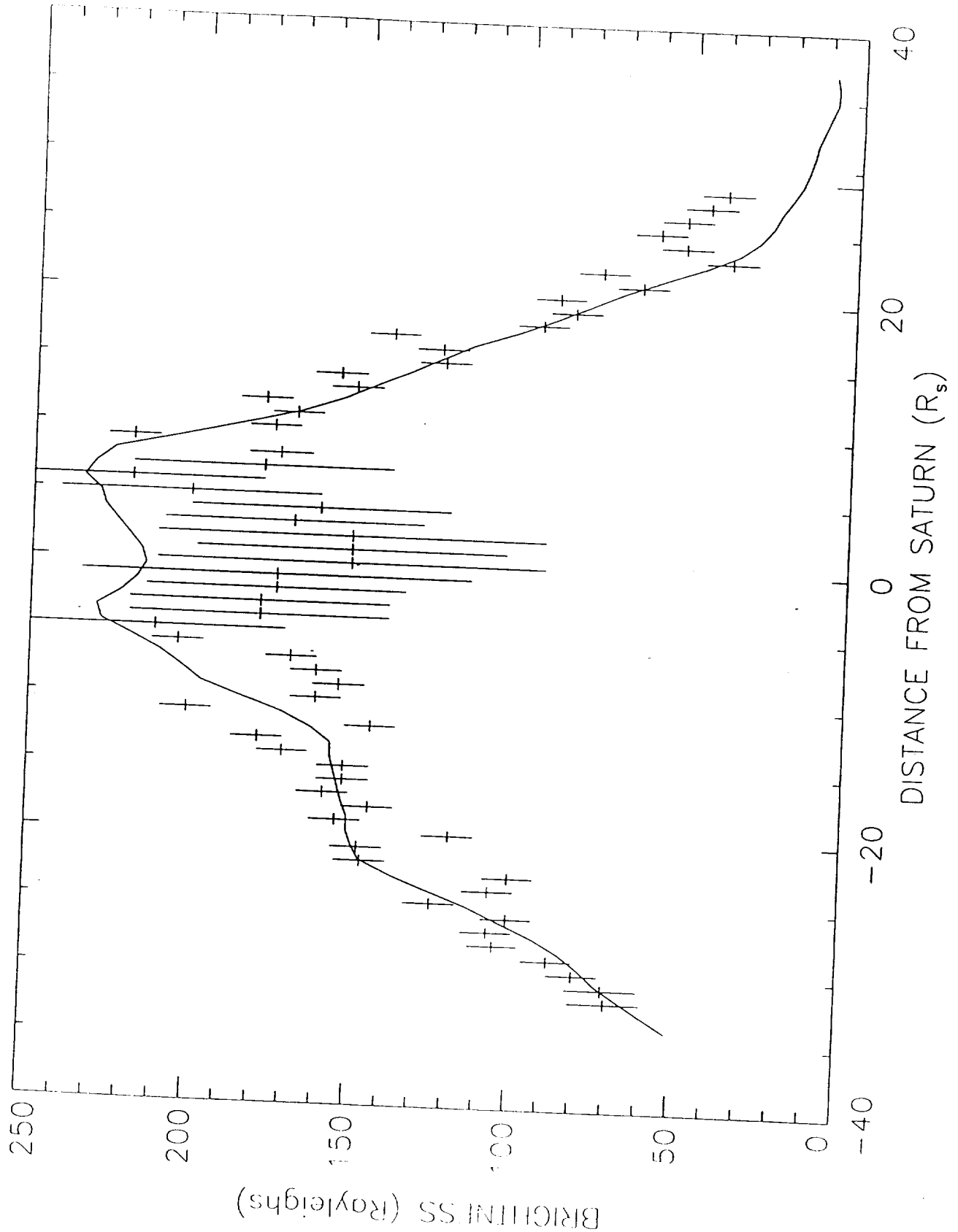
BRIGHTNESS (Rayleighs)
250
200
150
100
50
0
-40
-20
0
20
40
DISTANCE FROM SATURN ($R_s$)

Figure 3

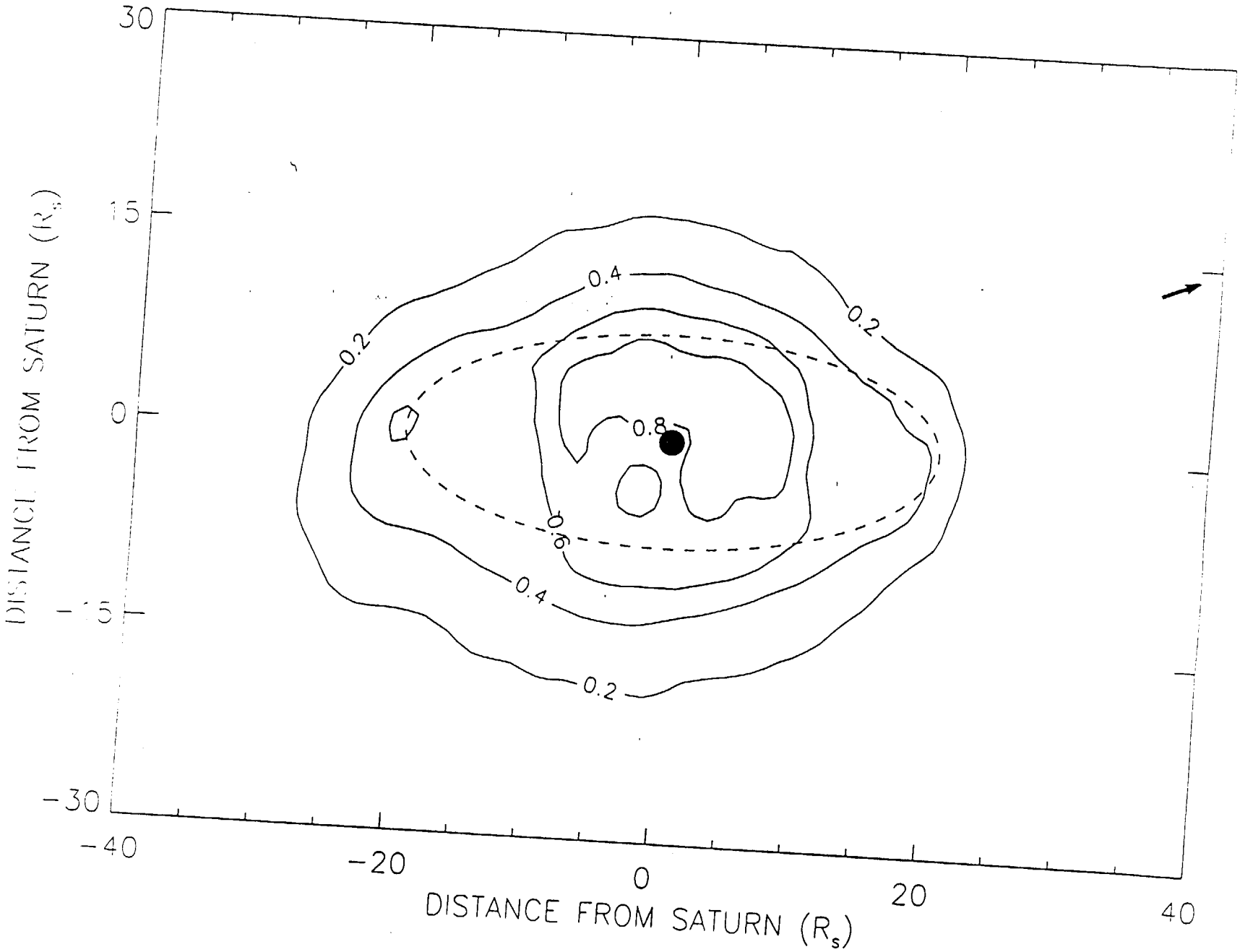
30
15
0
-15
-30
-40
-20
0
20
40
DISTANCE FROM SATURN ($R_s$)
DISTANCE FROM SATURN ($R_s$)
0.8
0.6
0.4
0.2
0.4
0.2
0.2

Figure 5

Figure 6

# REPORT DOCUMENTATION PAGE

Form Approved
OMB No. 0704-0188



| 1. AGENCY USE ONLY (Leave blank) | 2. REPORT DATE | 3. REPORT TYPE AND DATES COVERED |
|---|---|---|
| | July 1997 | Final Jan. 24, 1994 to July 23, 1997 |

**4. TITLE AND SUBTITLE**

Studies of the Gas Tori of Titan and Triton

**5. FUNDING NUMBERS**

NASW-4832

**6. AUTHOR(S)**

William H. Smyth and M. L. Marconi

**7. PERFORMING ORGANIZATION NAME(S) AND ADDRESS(ES)**

Atmospheric and Environmental Research, Inc.
840 Memorial Drive
Cambridge, MA 02139

**8. PERFORMING ORGANIZATION REPORT NUMBER**

P-498

**9. SPONSORING/MONITORING AGENCY NAME(S) AND ADDRESS(ES)**

NASA Headquarters
Headquarters Contract Division
Washington, DC 20546

**10. SPONSORING/MONITORING AGENCY REPORT NUMBER**

**11. SUPPLEMENTARY NOTES**

**12a. DISTRIBUTION/AVAILABILITY STATEMENT**

**12b. DISTRIBUTION CODE**

**13. ABSTRACT** *(Maximum 200 words)*

A model for the spatial distribution of hydrogen in the Saturn system including a Titan source, an interior source for the rings and inner icy satellites, and a Saturn source has been applied to the best available Voyager 1 and 2 UVS Lyman-$\alpha$ observations presented by Shemansky and Hall (1992). Although the model-data comparison is limited by the quality of the observational data, source rates for a Titan source of 3.3 - 4.8x$10^{27}$ H atoms $s^{-1}$ and, for the first time, source rates larger by about a factor of four for the interior source of 1.4 - 1.9x$10^{27}$ H atoms $s^{-1}$ were determined. Outside the immediate location of the planet, the Saturn source is only a minor contribution of hydrogen. A paper describing this research in more detail has been submitted to The Astrophysical Journal for publication and is included in the Appendix. Limited progress in the development of a model for the collisional gas tori of Triton is also discussed.

**14. SUBJECT TERMS**

**15. NUMBER OF PAGES**
57

**16. PRICE CODE**

| 17. SECURITY CLASSIFICATION OF REPORT | 18. SECURITY CLASSIFICATION OF THIS PAGE | 19. SECURITY CLASSIFICATION OF ABSTRACT | 20. LIMITATION OF ABSTRACT |
|---|---|---|---|
| Unclassified | Unclassified | Unclassified | |